Chapter 4
Flood Risk Assessment of Himalayan Foothill Rivers: A Study of Jaldhaka River, India

Adrija Raha, Suraj Gupta, and Mery Biswas

Abstract Flood is an annual recurrent event in the Himalayan foothill province of West Bengal. The middle course of Jaldhaka River basin experiences flood occasionally. The main river with its tributaries carries huge discharge during monsoon periods, resulting floods that affect the entire landscape. The study is an assessment of flood susceptibility using analytical hierarchy process (AHP) where elevation (m), slope (degree), mean rainfall (cm), normalized difference vegetation index (NDVI), bare soil index (BSI), topographic wetness index (TWI), and distance from rivers (km) have been considered. Five classes have been assessed where very high and high flood susceptibility areas are concentrated in the lower flood plain section of Rothikhola, Sukti, and Jaldhaka itself. There is remarkable changes from 2000–2020 in land utilization also where settlement and agricultural land have increased enormously in moderate to low flood-risk sections of near-foothill area and settlement has shifted from the flood plains to the northern section. Natural vegetation has decreased, and there is a remarkable increase of agricultural land over both banks of river channels. The outcome of the study portrays a change in the land utilization pattern affected by recurrent flood events.

Keywords Himalayan foothill · AHP · Flood susceptibility · LU/LC change

1 Introduction

Flood is one of the destructive natural hazards, which causes huge loss to human life, property, infrastructure, agricultural lands, and much irreversible damages (Swain et al., 2020). It causes overall disruption to the development activity and the daily economic practice of people (Zhong et al., 2018; Yésou et al., 2013; Patrikaki et al., 2018; Birkholz et al., 2014; Mouratidis & Sarti, 2012; Astaras et al., 2011; Domakinis et al., 2020). Among the hydrometeorological disasters, flood is

A. Raha · S. Gupta · M. Biswas (✉)
Department of Geography, Presidency University, Kolkata, West Bengal, India
e-mail: mery.geog@presiuniv.ac.in

considered as the most destructive natural hazard, accounting for 43.5% of death (Ahmed et al., 2021; CRED, 2015; Hu et al., 2018; Li et al., 2016). It has been surveyed that 170 million people get affected annually by this natural hazard (Kowalzig, 2008). The economic challenges are much greater for developing and underdeveloped countries (Quesada Román, 2021). Therefore, it is of utmost importance to focus on flood risk management programs and to overcome national boundaries, socioeconomic limitations, and geographical locations (Degiorgis et al., 2012; Kazakis et al., 2015). Due to rapid urbanization and developmental activity as well as other human interventions like deforestations, natural hazards like floods are becoming frequent and devastating as well. Deforestation, unplanned urbanization, change in land use and land cover, faulty agricultural practices, and climate change are some of the important factors responsible for the increasing frequency of flood occurrence (Quesada Román, 2021; Jarrett & Tomilson, 2000; Chang & Franczyk, 2008). Along with these factors, the characteristics of river basins can also play a major part in the occurrence of floods (Mohamed & El-Raey, 2019; Bhat et al., 2019; Ahmed et al., 2021). With the evolution of different methodologies, the approach to flood management has been changed (Das & Sahu, 2017). The nonstructural methods for flood risk management are gaining popularity, which encompasses forecasting of floods, flood susceptibility mapping, and flood inundation mapping. The application of remote sensing and geographical information system have provided updated tools, which are helpful for preparing flood susceptibility maps and for assessing the flood hazard risk more accurately (Sankhua et al., 2015; Rai & Mohan, 2014; Ahmad, 2018; Sahu, 2014), and have provided a reliable decision-making tool for the management of flood risk (Dewan, 2013; Ahmed et al., 2021; El Bastawesy et al., 2019; Mohamed & El-Raey, 2019; Shehata & Mizunaga, 2018; Youssef et al., 2015). The incorporation of certain factors like meteorology, geomorphology, topography, lithology, geology, and land use pattern with the help of geographic information system can provide a detailed account of the flood risk zonation (Das & Sahu, 2017, Biswas & Dhara, 2019). The global coverage of remote sensing data and its accessibility have helped to monitor the flood hazard more accurately (Baez-Villanueva et al., 2018; Zhao et al., 2014; Paul et al., 2019). The approach of integration of remote sensing and geographic information system along with morphological and meteorological analysis is being used significantly for the assessment of flood hazard zonation (Kabenge et al., 2017; Mahmood & Rahman, 2019; Rastogi et al., 2018). It has also become a helpful management tool to delineate flood susceptibility zones (Adnan et al., 2019; Dawod et al., 2012; Mahmood & Rahman, 2019; Sarkar & Mondal, 2019; Youssef et al., 2010). Analytical hierarchy process (AHP) (Chakraborty & Joshi, 2014; Dandapat & Panda, 2017; Kazakis et al., 2015), frequency ratio (FR) model (Sarkar & Mondal, 2019), machine learning, multi-criteria decision model (MCDM) (Costache et al., 2019; Khosravi et al., 2016; Rahman et al., 2019), and flow model (FM) simulation (Baky et al., 2019) are some popular and cost-effective approaches to prepare flood susceptibility maps.

In the case of India, due to the unpredictable and uncertain activity of summer monsoon, numerous events of catastrophic flood are witnessed (Roy et al., 2021; Dhar & Nandagri, 2003). In the areas where much of the rainfall happens between June and September, during the summer monsoon, floods are considered to be a perpetual natural disaster (Roy et al., 2021). Therefore, this season is a matter of concern, as around 32 million citizens of India are vulnerable to flood risk (Kale, 2004).

The Himalayan foreland in West Bengal is drained by numerous rivers with a general flow direction toward the south and southeast (Raha & Biswas, 2022a, b). These rivers have largely shaped the foreland portion with its huge sediment deposition, which is associated with monsoonal rainfall and discharge fluctuations. The rise in the river water level is dependent upon the spatial distribution of rainfall, its duration, and intensity (Roy, 2011; Paul & Biswas, 2019; Biswas & Banerjee, 2018). In the upper catchment areas of the rivers, occasional landslide events perpetuate into sudden bursting of water, which eventually makes the river channels release massive volumes of water, as it happened in the case of Teesta River in 1968 (Roy, 2011). Teesta, Leesh, Gheesh, Chel, Neora, Muri, Jaldhaka, Diana, Rohtikhola, and Sukti are some of the major rivers that flow through Jalpaiguri and Alipurduar. The Jaldhaka River's middle course, as well as its tributaries, experience extensive flooding, particularly in the lower course. It is associated with excessive rainfall, slope, flow behavior, etc., which makes the rivers unpredictable (Ghosh, 2018). Therefore, the objectives of the study are to analyze the flood susceptibility zones considering certain parameters and to understand the effects of flood inundation on different land use and land cover and its consequential changes.

2 Study Area

One of the main rivers of the Himalayan Foothill region in West Bengal is River Jaldhaka. A report provided by the North Bengal Flood Control Commission, North Bengal (NBFCC) (1965) based on the Gauge Height of various rivers at various time periods indicated the flood-prone nature of the rivers (Table 4.1). The Himalayan foreland region in West Bengal (Fig. 4.1) is endowed with River Jaldhaka and its tributaries like Murti, Jiti, Khuji Diana, Diana, Rohtikhola, and Sukti, which are considered to be flood prone. The area under consideration has an area of 1745.4 km^2 extending from River Murti in the West to River Sukti in the East, from the Himalayan Mountain front in the north to the confluence of Jaldhaka and Sukti in the South. The focus on flood risk zonation of the considered study area is of utmost importance as the area forms the riparian parts of the sub-Himalayas where maximum number of rivers have a common source (Chakraborty & Mukhopadhyay, 2019; Ghosh & Kar, 2018). In the varying nature of climatic components, high amount of annual rainfall has contributed to the flood susceptibility of the area (Table 4.2) (Mandal & Sarkar, 2016; Shrestha et al., 2012; Roy, 2011). Though

Table 4.1 Flood and nonflood event in different rivers in the district (Das et al. 2017)

Rivers	Floods	Nonfloods	Observation year
Teesta	14	9	23
Jaldhaka	18	8	26
Diana	7	8	15
Torsa	14	1	15
Raidak I	11	4	15
Raidak II	6	9	15
Kaljani	9	6	15
Sankosh	5	10	15
Mujnai	8	7	15
Jainti	12	3	15
Dharala	11	4	15
Neora	7	9	16

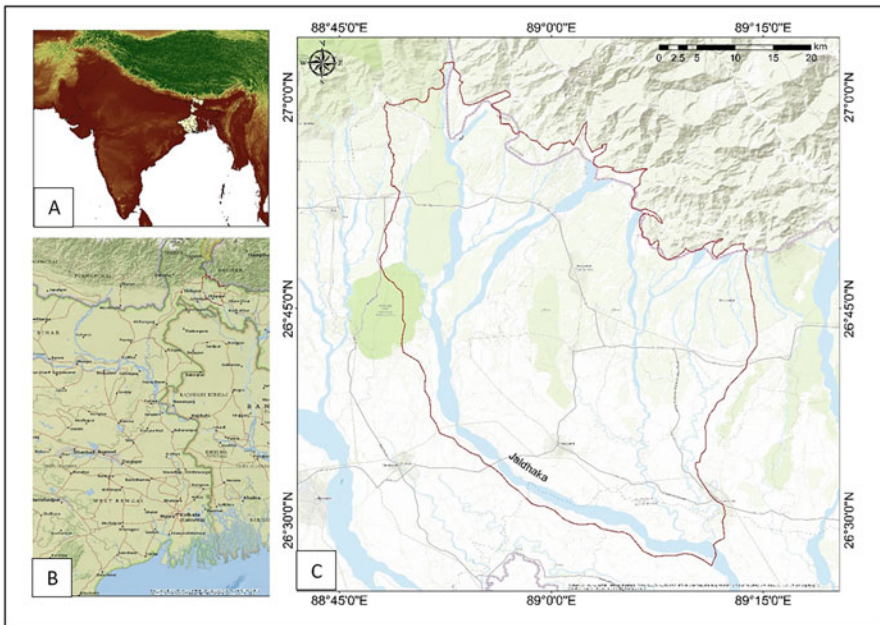Source: NBFCC (North Bengal Flood Control Commission)

Fig. 4.1 (**a–c**) Location of the considered study area with Jaldhaka and its tributaries

inundation is a very common and frequent phenomenon, the intensity and damage potentials vary spatially depending upon the areal extent of inundation, the total number of population affected, loss of life, livelihood, properties, and damages to the infrastructures (Das et al., 2017).

Table 4.2 Previous records of rise in gauge height of River Jaldhaka (Gauge station: NH-31 Crossing)

| Year | Maximum water level/flood peak | | One day maximum rainfall (mm) |
	On	Remarks	
2020	11.07.2020	0.13 M above DL	222.0
2018	10.09.2018	0.15 m. above DL	300.0
2017	12.08.2017	0.11 m above DL	216.00
2015	07.06.2015	0.10 m above DL	Data not available
	23.06.2015	0.11 m above DL	
	02.09.2014	0.85 m above DL	
2012	17.06.2012	0.05 m above DL	
	16.07.2012	0.25 m above DL	
2009	20.08.2009	0.28 m above DL	
2008	06.07.2008	0.09 m above DL	
2007	04.09.2007	0.11 m above DL	
	07.09.2007	0.30 m above DL	
2005	20.07.2005	0.23 m above DL	
2004	20.07.2004	0.20 m above DL	
2003	01.07.2003	0.13 m above DL	
	08.07.2003	0.14 m above DL	
2000	04.08.2000	0.10 m above EDL	
1998	26.08.1998	0.35 m above DL	
1996	13.07.1996	0.42 m above DL	

Annual Flood Report from 1991 to 2020, Irrigation and Waterways Directorate, Government of West Bengal
DL danger level, *EDL* extreme danger level

3 Data Used and Methodology

To execute the flood susceptibility zone, mapping of total seven parameters has been taken into consideration (Table 4.3). After literature review and thorough field investigations, these parameters have been considered to be applicable in the region. Authors have considered these parameters to be suitable for susceptibility mapping. Other parameters could have been applied if the study area was larger.

3.1 Elevation

The altitudinal attribute of any region plays an important role to understand the probability of flooding in that region. It is important to note that flat lands and low-lying regions are more prone to flood hazards as the water flows down from high altitudinal zone to lowland areas causing stagnation of water for a significantly long period of time, which ultimately leads to flood-like situation, that is inundation of the land (Tehrany et al., 2014).

Table 4.3 Parameters selected for preparing flood susceptibility map

Parameters	Elevation (meter)	Slope (degree)	Normalized Difference Vegetation Index (NDVI)	Topographic Wetness Index (TWI)	Bare Soil Index (BSI)	Mean rainfall (cm)	Distance from rivers (km)
Formula and details	Classified into five classes based on Digital Elevation Model in ArcGIS 10.4.1	Processed from DEM in ArcGIS 10.4.1 following the steps: **3D Analyst Tool** →**Raster Surface** →**Slope (Degree)**	$\frac{NIR-R}{NIR+R}$ Where, NIR = Near Infrared R=Red	$\ln\left(\frac{As}{\tan\beta}\right)$ Where, As = Flow Accumulation Tanβ= Surface slope gradient	$\frac{(SWIR+R)-(NIR+B)}{(SWIR+R)+(NIR+B)}$ Where, NIR = Near Infrared R = Red B = Blue SWIR = Short Wave Infrared	Gridded data process in ArcGIS 10.4.1 to prepare mean rainfall map	Map has been prepared based on line density tool of ArcGIS 10.4.1
Data type	ASTER GDEM Version 3,30m × 30m	ASTER GDEM Version 3, 30m × 30m	Landsat 8 OLI/TIRS USGS, 30m × 30-m	ASTER GDEM Version 3, 30 m × 30 m	Landsat 8 OLI/TIR USGS, 30m × 30-m	High-resolution gridded data, 0.5 ° × 0.5° CRU TS v. 4.04 (Climatic Research Unit gridded Time Series) version 4	Geological survey of India (GSI) data, 1:50,000
Source of data	https://search.earthdata.nasa.gov	https://search.earthdata.nasa.gov	https://search.earthdata.nasa.gov	https://search.earthdata.nasa.gov	https://search.earthdata.nasa.gov	https://sites.uea.ac.uk/cru/data	https://www.gsi.gov.in

3.2 Slope

Slope is a significant factor of flood susceptibility mapping as it determines the flow of river water and runoff. It is noted that areas of flat slope disrupt the natural flow of water, which perpetuates into the stagnation of water, thus leading to flood-hazard risk (Bui et al., 2019). The infiltration rate is directly related to the topographic slope (Das, 2019). The steep gradient of land hinders infiltration of rainwater.

3.3 Rainfall

The flood hazard risk is largely dependent upon the duration and intensity of rainfall of a particular region. The rainfall characteristics of the study area is influenced by the south-west monsoon wind. The location of the study area as a Himalayan foreland makes it receive heavy rain as the Himalayan orogenic belt acts as a barrier, which intercepts the monsoon wind and causes huge rainfall between the month of June to September (Roy et al., 2021). The duration and intensity of rainfall directly influence the flood susceptibility of an area. With the increasing intensity of rainfall, the flood hazard risk also increases (Rozalis et al., 2010; Mirzaei et al., 2020).

3.4 Distance from Rivers

Previous researchers (Tien Bui et al., 2019) have considered distance from rivers to be a significant factor determining the risk of flood hazard. The heavy rainfall increases the discharge amount of the rivers exceeding their carrying capacity. Thus, the areas near the rivers are more prone to flood hazards. Numerous researches have provided the threshold distance from the rivers, which are more susceptible to flooding. Samanta et al. 2016 has considered less than 100 m from the rivers to be most susceptible to flooding. Pradhan 2009 has observed that a distance less 90 m from the rivers is prone to flood hazard risk.

3.5 Normalized Difference Vegetation Index (NDVI)

NDVI is a dimensionless index, which ranges between +1 and − 1 where the dense vegetation represents values near +1. Vegetation cover largely affects flood susceptibility and intensity of flood risk hazard as there is a negative correlation between vegetation density and flood hazards (Mojaddadi et al., 2017; Rahman et al., 2019; Kaur et al., 2017).

3.6   Bare Soil Index (BSI)

The bare soil index indicates the bare regions, which have nearly no vegetation cover and thus are susceptible to flood risk. The bare soil cover facilitates runoff decreasing the infiltration rate, therefore increasing the flood risk.

3.7   Topographic Wetness Index (TWI)

Topographic wetness index is a useful parameter to understand the extent of flood susceptible zone. Previous researches have analyzed the fact that if the value of TWI exceeds a threshold for a part of the watershed, the area is supposed to be saturated (Woods & Sivapalan, 1997; Alam et al., 2021). The index helps to delineate the extent of the watershed, which is likely to get inundated after heavy rainfall.

Each parameter has been classified into five classes. Analytical hierarchy process (AHP) has been adopted to give (Table 4.4) the parameters weightage. AHP is a significant tool that takes into account multiple variables in GIS platform for decision-making (Şener et al., 2010). This technique was introduced by Saaty (1980, 1990) to assign weightage to the parameters based on some indicators to make a structure, which is hierarchical in nature. Consistency Index (CI) is calculated:

$$CI = \frac{\gamma Max - n}{n - 1} \tag{4.1}$$

$$CR = CI - RI \tag{4.2}$$

Table 4.4 Pairwise comparison matrix and weightages of the parameters assigned using AHP

	Rainfall	Elevation	Slope	NDVI	BSI	SAVI	Distance from river	Weightage
Rainfall	1	2	2	3	3	4	5	0.285499
Elevation		1	2	3	3	4	5	0.234821
Slope			1	3	3	4	4	0.189104
NDVI				1	2	3	4	0.111195
BSI					1	3	4	0.0914571
TWI						1	3	0.0538256
Distance from River							1	0.0340976
Maximum eigen value = 7.45045								
Consistency index = 0.0750754								
Consistency ratio (consistency index/random consistency index) = 0.0750754/1.35 = 0.055611407								

Table 4.5 Accuracy Assessment for LULC, 2000 using kappa coefficient, where overall accuracy is 95.62%

	River	Agriculture	Vegetation	Built-up	Barren land	Water body	Total (user)
River	21	0	0	0	0	0	21
Agriculture	0	32	1	1	0	0	34
Vegetation	0	1	59	0	0	0	60
Built-up	0	0	1	19	2	0	22
Barren land	0	0	0	0	9	0	9
Water body	0	0	0	1	0	13	14
Total (producer)	21	33	61	21	11	13	**160**

$$\text{Overall accuracy} = \frac{\text{Total Number of Correctly Classified Pixels (Diagonal Elements)}}{\text{Total Number of Reference Pixels}} \times 100$$
$$= \frac{153}{160} \times 100$$
$$= 95.625\%$$

$$\text{Kappa coefficient } (\text{K}) = \frac{(TS \times TCS) - \sum(\text{Column Total} \times \text{Row Total})}{(TS)^2 - \sum(\text{Column Total} \times \text{Row Total})} \times 100$$
$$= \frac{[(160 \times 153) - \{(21 \times 21) + (33 \times 34) + (61 \times 60) + (21 \times 22) + (9 \times 11) + (14 \times 13)\}]}{[(160)^2 - \{(21 \times 21) + (33 \times 34) + (61 \times 60) + (21 \times 22) + (9 \times 11) + (14 \times 13)\}]} \times 100$$
$$= \frac{[24480 - 5966]}{[25600 - 5966]} \times 100$$
$$= \frac{18514}{19634} \times 100$$
$$= 94.29\%$$

Here CI is consistency index, CR is consistency ratio, RI is random consistency index, γMax is computed average value of weight, and *n* is the number of parameters. There is a randomly generated comparison matrix according to Satty scale. CR has been computed to check the consistency of the judgment matrix. As per the Satty scale, for CR ≤ 0.10, the matrix can be marked with satisfactory consistency.

Land use/land cover maps for 2000 and 2020 have been prepared to understand the impact of flood hazard on different land use patterns. The land use maps have been prepared based on Landsat 4–5 and Landsat 8 data. Landsat 4–5 Thematic Mapper (TM) images consist of seven spectral bands with a spatial resolution of 30 meters for Bands 1–5 and 7. Spatial resolution for Band 6 (thermal infrared) is 120 meters but is resampled to 30-meter pixels. The approximate scene size is 170 km north-south by 183 km east-west (106 mi by 114 mi). The used Landsat 8 data is 30 m spatial resolution having 11 bands. It is under UTM projection system of zone 45 and WGS84 ellipsoid. Accuracy assessment (Tables 4.5 and 4.6) has been performed to verify the reliability of the classification using Kappa coefficient. According to the kappa coefficient in 2000, over all accuracy is 95.26% and kappa coefficient (#x049A) is 94.29%. It has also calculated in 2020 LUSC map where 98.12% is overall and 97.64% is kappa coefficient (K).

Table 4.6 Accuracy assessment for LULC, 2020 using kappa coefficient, where overall accuracy is 98.12%

	River	Agriculture	Vegetation	Built-up	Barren land	Water body	Total (user)
River	18	0	0	0	0	0	18
Agriculture	0	41	1	0	0	0	42
Vegetation	0	1	46	0	0	0	47
Built up	0	0	1	24	0	0	25
Barren land	0	0	0	0	15	0	15
Water body	0	0	0	0	0	13	13
Total (producer)	18	42	48	24	15	13	**160**

$$\text{Overall accuracy} = \frac{\text{Total Number of Correctly Classified Pixels (Diagonal Elements)}}{\text{Total Number of Reference Pixels}} \times 100$$
$$= \frac{157}{160} \times 100$$
$$= 98.125\%$$

$$\text{Kappa coefficient (K)} = \frac{(\text{TS} \times \text{TCS}) - \sum(\text{Column Total} \times \text{Row Total})}{(\text{TS})^2 - \sum(\text{Column Total} \times \text{Row Total})} \times 100$$
$$= \frac{[(160 \times 157) - \{(18 \times 18) + (42 \times 42) + (48 \times 47) + (24 \times 25) + (15 \times 15) + (9 \times 9)\}]}{[(160)^2 - \{(18 \times 18) + (42 \times 42) + (48 \times 47) + (24 \times 25) + (15 \times 15) + (9 \times 9)\}]} \times 100$$
$$= \frac{[25120 - 5250]}{[25600 - 5250]} \times 100$$
$$= \frac{19870}{20350} \times 100$$
$$= 97.64\%$$

4 Results

4.1 Elevation

The overall altitudinal pattern of the region is important to understand the areal extent of flood susceptible zones. The elevation of the considered study area has been classified under five classes – very high altitude (427–536 m), high altitude (317–426 m), moderate (207–316 m), gentle (97–206 m), and flat (50–96 m) (Fig. 4.2). The moderate altitudinal zone corresponds to the alluvial fan area of the foothill region whereas the gentle altitudinal zone corresponds with distal fan portions. The flat land in the southern-most part of the study area has been marked with several meandering rivers.

4.2 Slope

The slope of the entire region has been mapped categorizing into five classes – very steep slope (12.22–55.14 degree), steep slope (3.71–12.21 degree), moderate slope (2.03–3.7 degree), gentle slope (1.69–2.02 degree), and flat land (0–1.68 degree) (Fig. 4.3). It is noticed that the southern part of the study area is characterized by flat
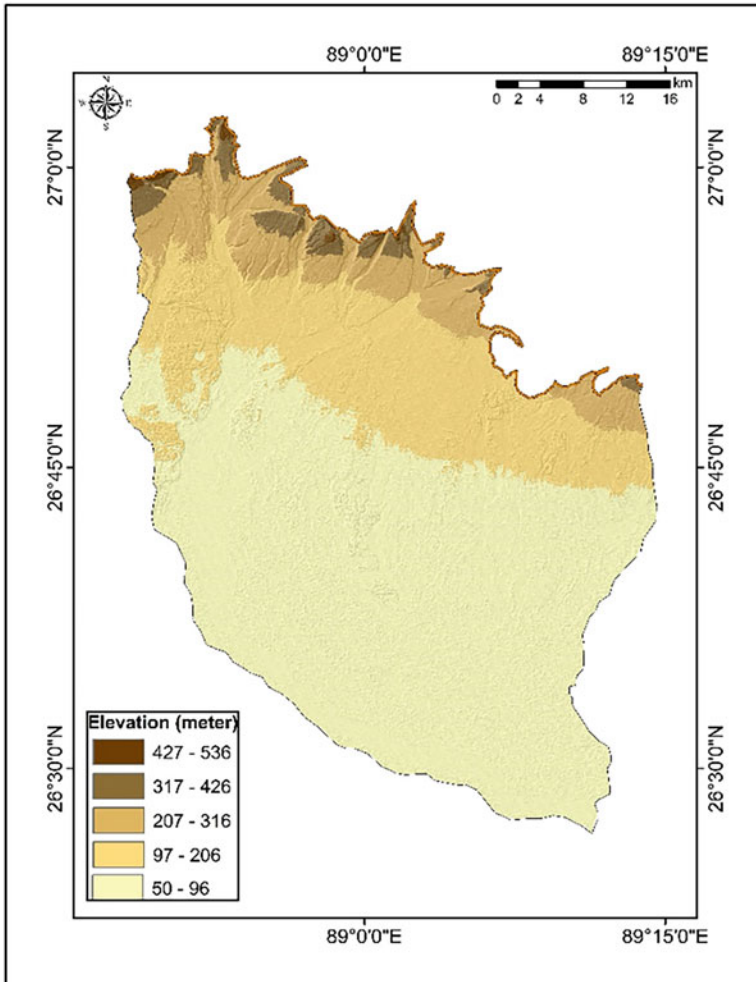
Fig. 4.2 Elevation map showing the altitudinal variation of the entire study area

land topography with very gentle slopes where the rivers have been characterized as meandering. On the other hand, in the frontal zone of the Himalayas, forested areas (Chapramari Reserve Forest, Maraghat Forest) have steep slopes.

4.3 Rainfall (Cm)

The mean rainfall map has been prepared based on five classes: class 1 (285.9–288.3 cm), class 2 (283.5–285.8 cm), class 3 (281.0–283.4 cm), class
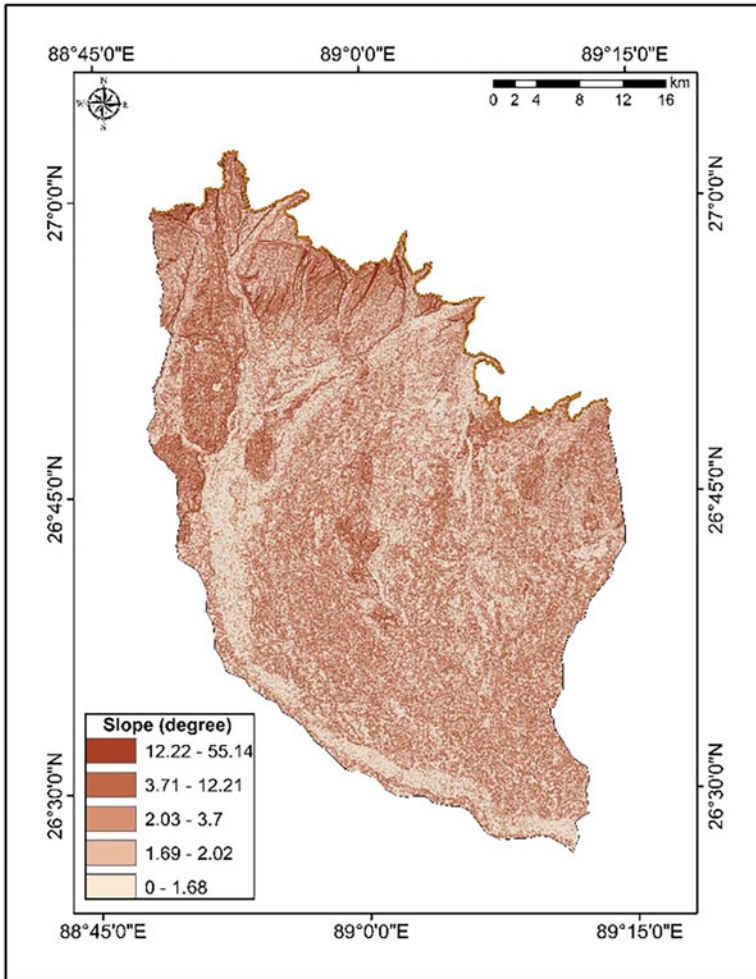
Fig. 4.3 Five classes of slope differentiation

4 (278.4–280.9), and class 5 (273.4–278.3 cm). It is to be noted that the eastern part of the map, which is drained by rivers Rohtikhola and Sukti, is receiving maximum amount of rainfall (285.9 cm). The amount of rainfall is decreasing from the eastern part of the area to the western part, which is drained by river Murti (Fig. 4.4).

5 Distance from Rivers (Meter)

The distance from rivers has been classified into five classes: class 1 (0–223.68 m), class 2 (223.69–306.84 m), class 3 (306.85–530.51 m), class 4 (530.52–1132.11 m), and class 5 (1132.12–2750.16 m) (Fig. 4.5).
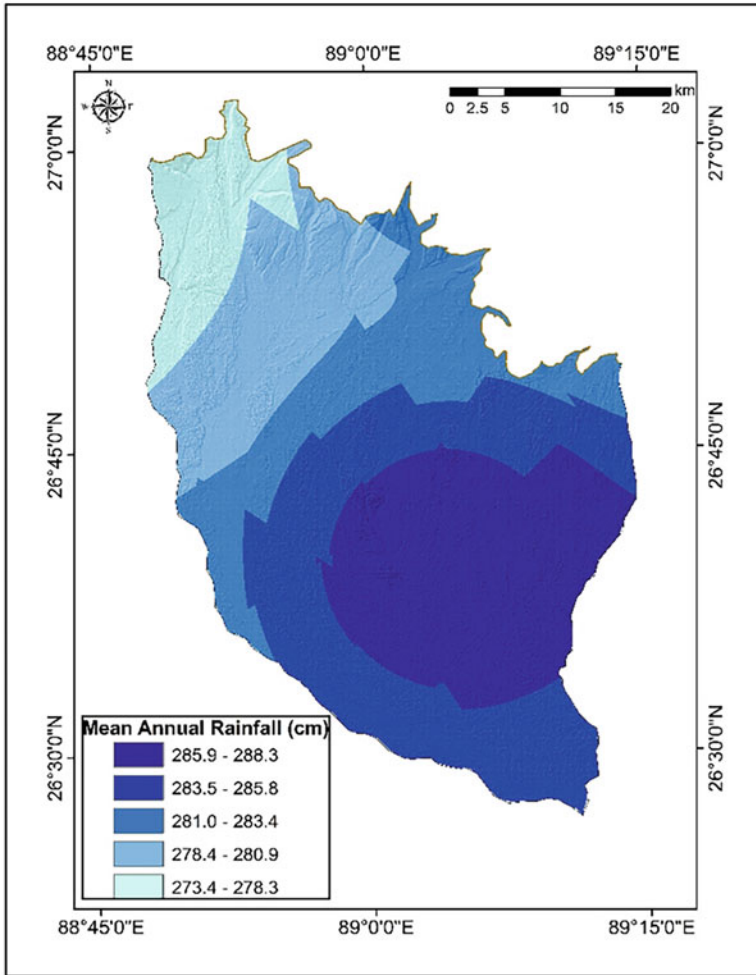
Fig. 4.4 Isohyet map of mean Rainfall of the study area

6   Normalized Difference Vegetation Index (NDVI)

In the considered study area, the maximum range of NDVI is 0.29–0.52, which corresponds to the dense forest region (part of Gorumara forest. Gairkata forest, Maraghat forest, and Chapramari.

Reserve forest) (Fig. 4.6). The agricultural plots of the alluvial fans including the tea gardens, which are on an elevated land, also represent higher values of NDVI (0.26–0.28). The southernmost part of the rivers represents very low value of NDVI, which indicates the bare land and less vegetation cover in that part.
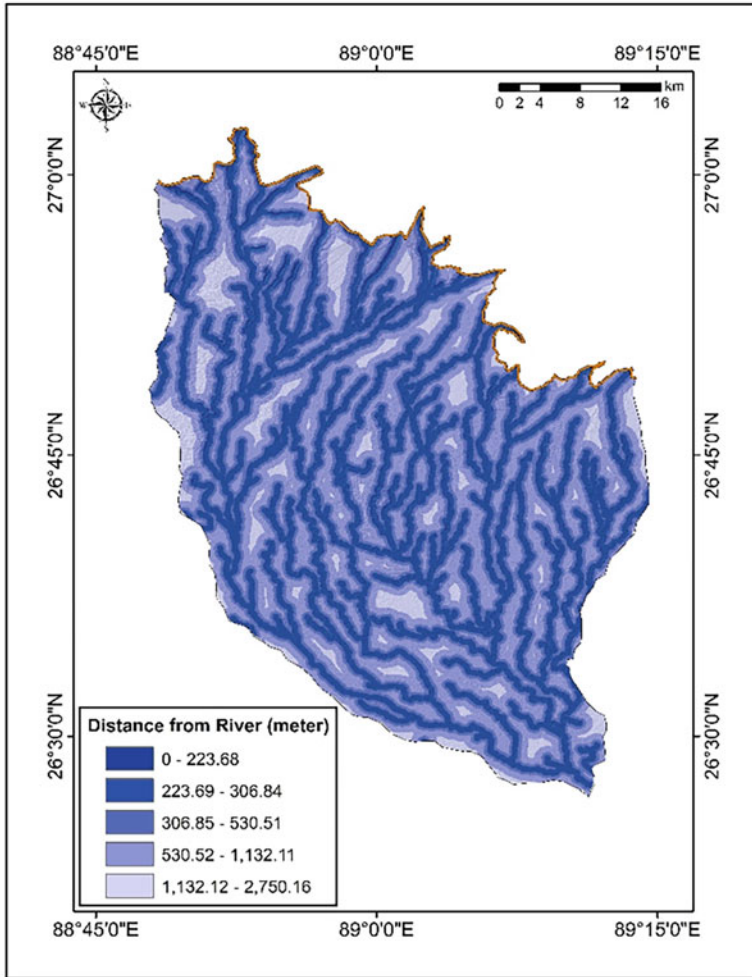
Fig. 4.5 Distance from River map showing five classes

7   Bare Soil Index (BSI)

Bare soil index has been classified into five classes: class 1 (0.01–0.14), class 2 (−0.04–0), class 3 (from −0.08 to −0.05), class 4 (from −0.12 to −0.09), and class 5 (from −0.28 to −0.13) (Fig. 4.7). The densely vegetated regions of the study area (part of Gorumara forest. Gairkata forest, Maraghat forest, and Chapramari Reserve forest correspond to lower values of BSI (from −0.28 to −0.13). The southern and western regions of the study area correspond to higher values of BSI (0.01–0.14), indicating less vegetation in the region.
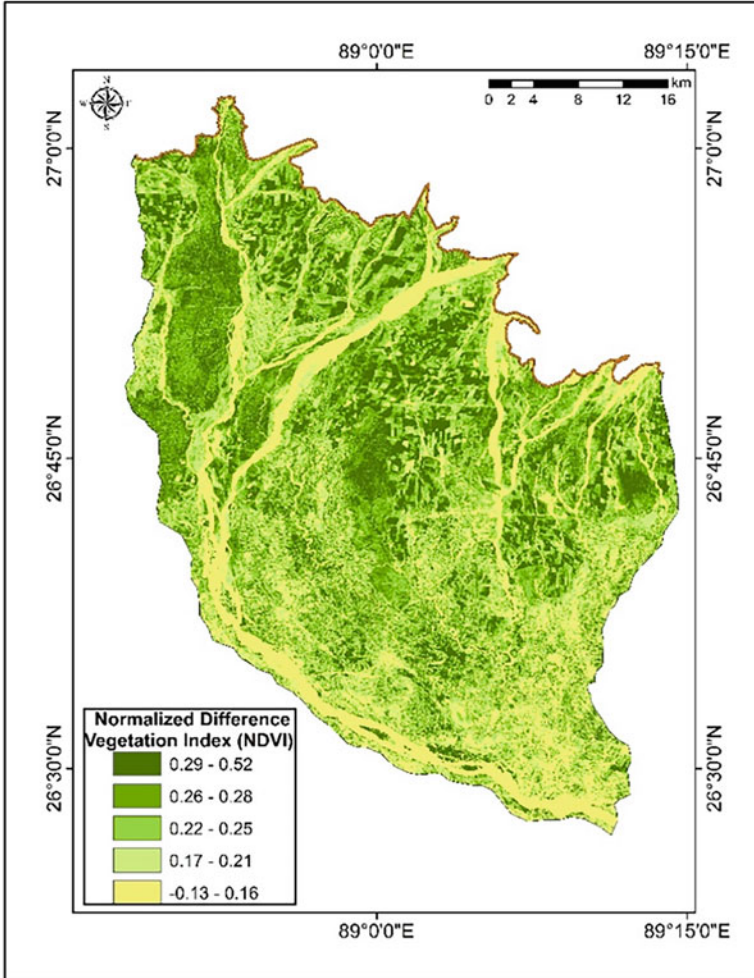
Fig. 4.6 Normalized Difference Vegetation Index (NDVI) map for visualizing 5 different classes of spatial distribution

8   Topographic Wetness Index (TWI)

TWI for the region has been classified into five classes: very high (12.55–18.06), high (9.03–12.54), moderate (6.78–9.02), low (5.35–6.77), and very low (3.09–5.34) (Fig. 4.8). It is to be noted that the areas in close proximity with the rivers portray higher values (12.55–9.03) of TWI.
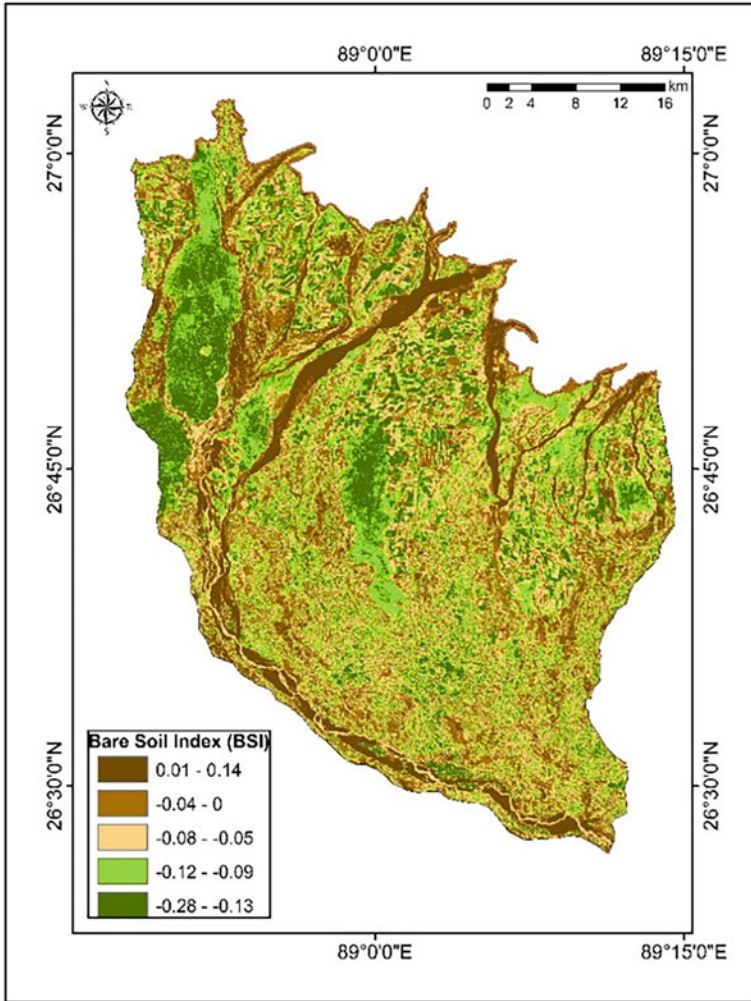
Fig. 4.7 Bare Soil Index (BSI) map of the study area

9 Flood Susceptibility Mapping

On the basis of the selected parameters, flood susceptibility map has been prepared, which has categorized the whole study area into five flood-susceptible classes (very high, high, moderate, low, and very low). Figure 4.9 portrays that the southern and western parts of the region specifically the region drained by rivers Rohtikhola and Sukti are very much susceptible to flood hazard risk. The narrow belt encircling the lower reaches of river Jaldhaka also seems to be susceptible to flood hazards. The region close to the higher reaches of the rivers is very less susceptible to flooding.
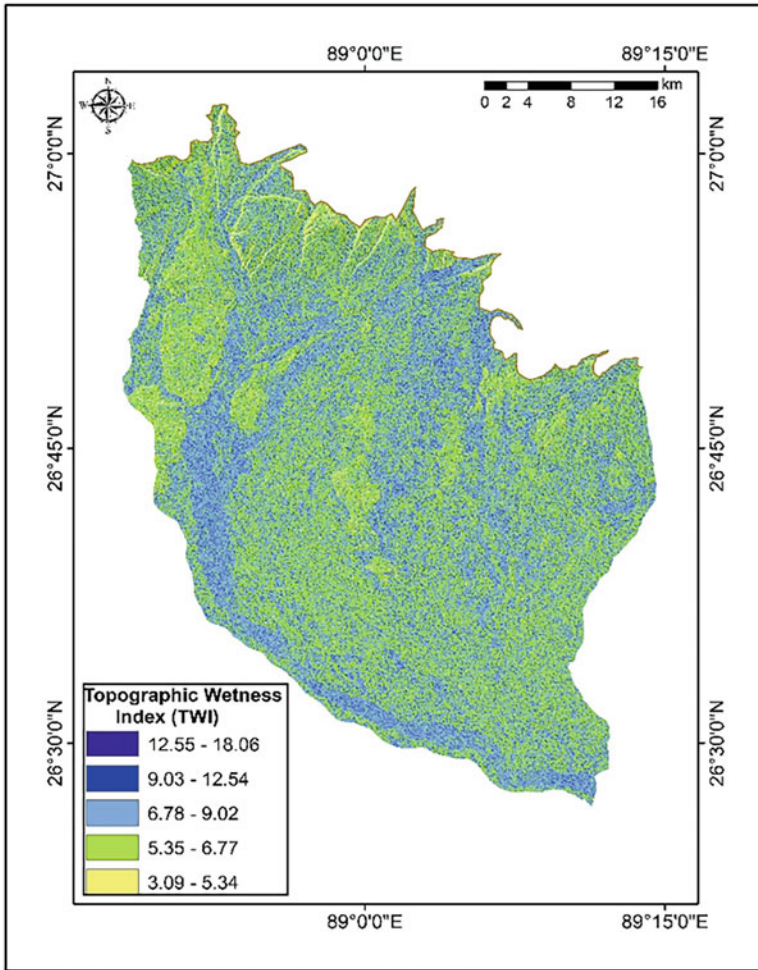
Fig. 4.8 Map of soil-adjusted vegetation index (SAVI)

9.1 *Validation*

It is of utmost importance to validate any model and to verify the outcome of the study. In spatial earth science, the multi-criteria decision making model can best be validated with the help of area under curve (AUC) as it verifies the outcome of the model with comprehensiveness and simplicity (Malik et al., 2020; Darabi et al., 2019).

To verify the present model regarding flood susceptibility, several flood inventory points have been used from the AUC analysis. Previous research works, official documents from the Irrigation and Waterways Department, Govt. of West Bengal
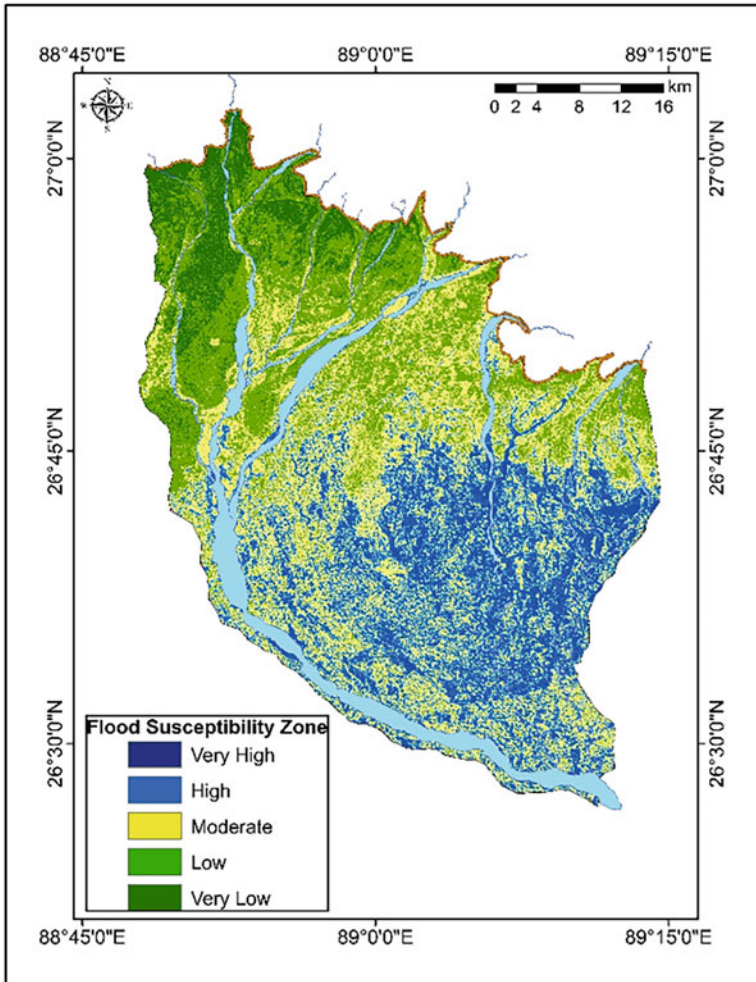
Fig. 4.9 Flood susceptibility map based on analytic hierarchic process (AHP)

(www.wbiwb.gov.in/), have been analyzed for the verification of the model with AUC.

Arabameri et al. (2019) and Rimba et al. (2017) have provided a classification of the accuracy of AUC curve as excellent (0.9–1.0), very good (0.80–0.90), good (0.70–0.80), poor (0.60–0.70), and weak (0.50–0.60). The computation of AUC has provided a value of 0.819 or 81.9%, which can be considered very good for the outcome of the model (Fig. 4.10).

Fig. 4.10 Validation of the flood susceptibility model using area under curve (AUC)
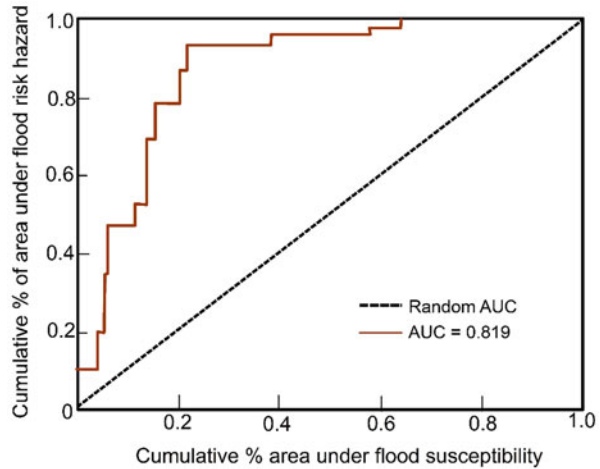
10   Discussion

The present study evaluates the flood susceptibility zonation by applying the multi-criteria decision method based on a combination of hydrological and geomorphic indices. The altitudinal zonation of the study area reveals the fact that the low elevated land in the southern part is mostly prone to flood risk hazard as the flat land creates stagnation of the rainwater during monsoon season.

The apex and distal part of alluvial fans having higher altitudes propagate easy flow of the rainwater (Raha & Biswas, 2022a, b). The gradient of the land portrays the probability of easy flow of river discharge and heavy monsoonal rainwater. The region in close proximity to the Himalayan Mountain front having steeper slope (12.22–55.14 degree) initiates easy and quick flow of river water, which in turn reduces the risk of flood hazard in the upper reaches of the rivers and adjoining areas. The very gentle sloping rolling topography encircling the middle and lower reaches of rivers Jaldhaka, Rohtikhola, and Sukti is vulnerable to flood hazard as the flood water during peak discharge of the rivers gets accumulated for a longer period of time. Moreover, the rivers Rohtikhola, Sukti, and their tributaries flow in a meandering pattern over the gently sloped land, which helps to propagate flood in this region as the velocity of river discharge decrease. The catastrophic rainfall in the region can be attributed as a major flood-controlling factor. The eastern part of the region drained by rivers Rohtikhola and Sukti is highly susceptible to flooding. Distance from rivers is also playing a significant role determining flood susceptibility. However, it is important to note that this parameter is playing crucial role in the lower and middle course of the rivers where the flood risk is dependent upon the higher order streams having greater volume of discharge.

The first-order and second-order streams that join the main Jaldhaka in foothill section have little or no significance in propagating flood-like situation as the volume of discharge is much less. But the main Jaldhaka river is fifth-order stream, and the

huge water during monsoon is carried by the catchment tributaries that cover
~1745.4 km^2. The vegetation cover seems to be a significant factor in controlling
flood hazards. Vegetation cover helps in the infiltration of water, and it is strongly
related with soil texture. The study area is mainly composed of sandy, sandy loamy
and clay soil, which has infiltration rate of 20–30 mm/hour, 10–20 mm/year and
1–5 mm/year, respectively (https://www.fao.org/3/s8684e/s8684e0a.htm)
(Fig. 4.11). The most flood susceptible zone is covered by sandy loam soil with
bare surface, where bare soil index value ranges from −0.04 to −0.08 and the
fluctuation of groundwater level (both rise and fall) is from 2–5 to 5–10 mbgl
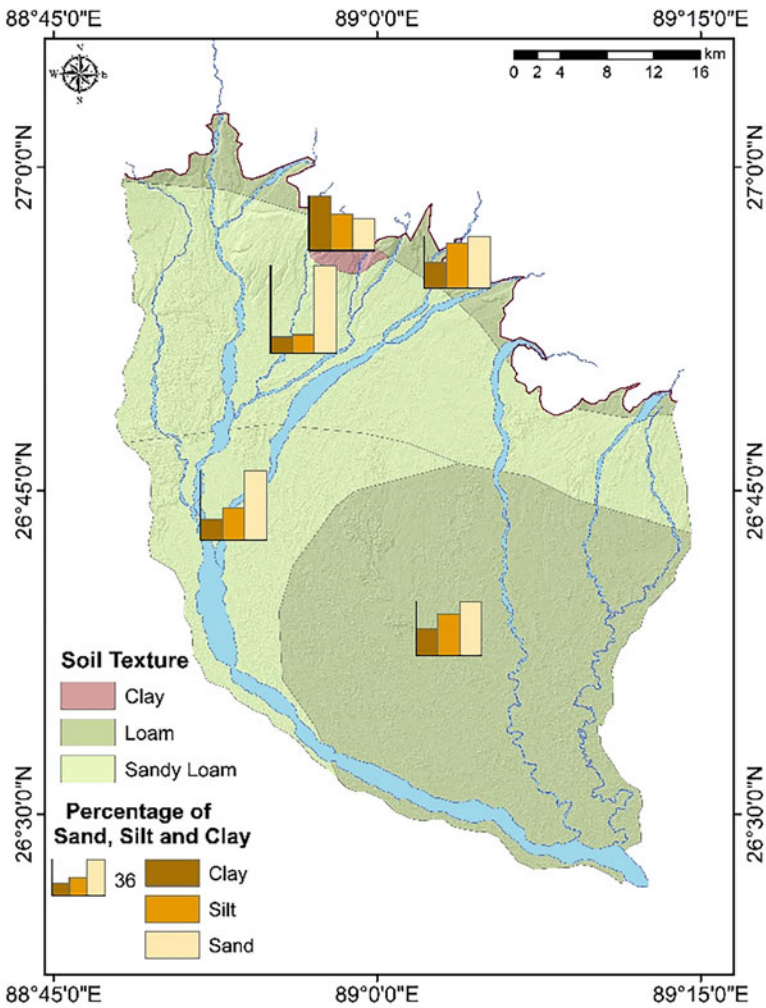

Fig. 4.11 Soil texture map and % of sand, silt and clay (based on Food and Agriculture Organization (FAO))

(central groundwater board, ministry of Jal Shakti, department of water resources, river development, and ganga rejuvenation government of India). Therefore, due to the infiltration, groundwater gets recharged seasonally. The dense vegetated areas are thus not susceptible to flooding (Kaur et al., 2017).

The bare surface of the southern part of the study area has lesser vegetation cover, which propagates flood hazard. It is interesting to note that among the different land use patterns (Fig. 4.12a–c), agricultural land and settlement are mostly affected by flood hazards. From 2000 to 2020 highest changes are found from vegetation to agricultural land (425.84 km^2) and vegetation to settlement (132.52 km^2). It specifies that vegetation has decreased and mostly been converted to agricultural land and settlement. These converted lands have increased the probability of flood as 40% of them are seasonally cultivated and exist as barren land that induce high run off rate. The higher susceptible is composed of sandy–loam soil, and the bareness of the lands insists it to be more prone to flood. Secondly, from 2000 to 2020, settlements have shifted toward the northern section due to flood in the lower Jaldhaka plains.

In the southeastern part of the study area, Khalaigram, East Dangapara, Salbari, and Malsagaon have been marked to be affected by frequent flood hazard. Construction of bridges and guide bunds also play an important role as during monsoon huge amount of water used to flow out through the narrow passage and in downstream water flashed out with high energy resulting flood and bank erosion. The comparison between the two land use maps enhances a significant outcome that the buildup area has been shifted and huge lands are transferred into an agricultural field, though it may be seasonally cultivated. Actually, these lands are most prone to be affected by floods in frequently.

Along with this, deaths of animals and people due to floods in the Himalayan foreland region also result in significant socioeconomic losses. Recurrent flooding affects a sizeable portion of the tea gardens and results in significant financial loss. After flood episodes, there is extensive sedimentation, which causes agricultural fields to lose fertility and production. Cropland flooding also destroys the agricultural output. A number of health problems are brought on by waterlogging in certain locations of Jalpaiguri, Alipurduar, and Cooch Behar. Building damage caused by bank failure is a frequent issue close to waterways.

Embankment breaches and spurs make the situation worse during a major flood. Occasionally, the percolation of dissolved minerals causes the quality of the groundwater to decrease. Taking an active, multidisciplinary approach is necessary for disaster management. Since the Himalayan foreland region experiences significant losses, flood management requires specific thought. Therefore, it is crucial to decrease flood threats' susceptibility. Building embankments along riverbanks can help shield the floodplain from repeated flooding episodes. Dykes and other structural control methods, such as spurs, may also be used. De-silting is a practical way to increase a river's carrying capacity in its lower sections, which can further aid to lessen flood susceptibility. To educate the general public about dangerous circumstances, community preparation is essential. Long-term watershed management should be implemented to reduce the negative consequences of flood episodes and to efficiently use the available natural resources.

Fig. 4.12 (**a**) Land use/land cover map of 2000 depicting major land use pattern in the study area. (**b**) Land use/land cover map of 2020 depicting major land use pattern in the study area. (**c**) Percentage wise change from one land use pattern to another land use pattern between 2000 and 2020
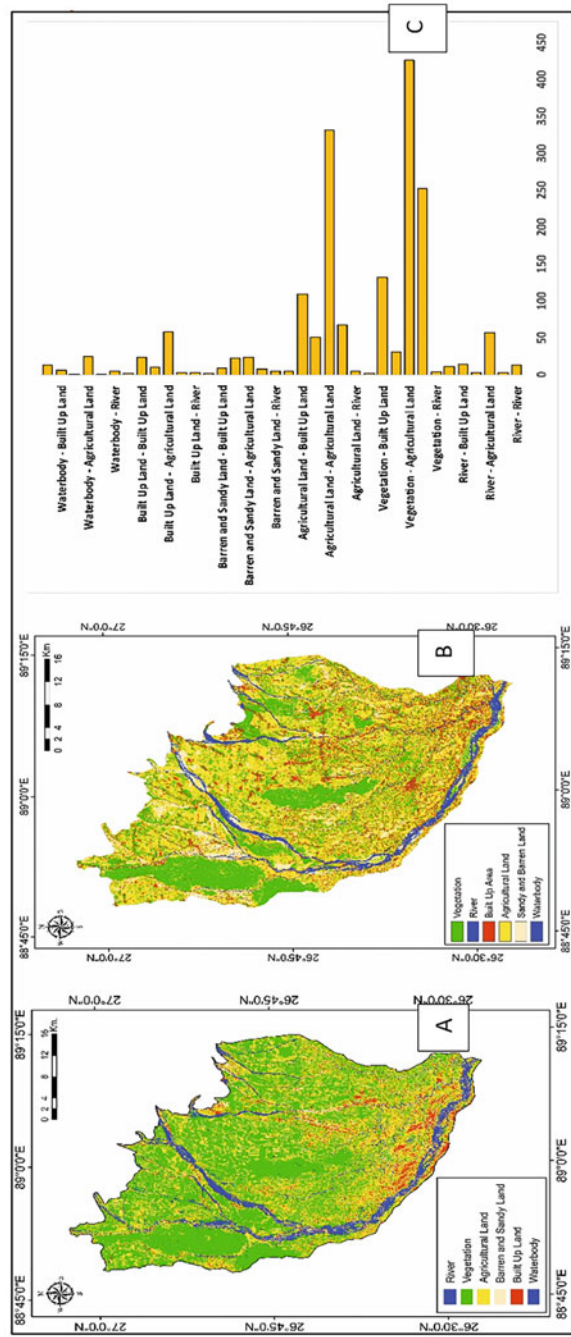
11 Conclusion

The whole flood plains of West Bengal's Jalpaiguri and Alipurduar districts have experienced flooding. Environmental degradation, such as forest fires, forest cutting, deforestation, soil erosion, and slope divergence, makes rivers more sensitive to disruption, including the area of the Jaldhaka River basin investigated. The flood susceptibility map shows that the lowest reaches of all riverine portions are prone to flooding. The LU/LC pattern has shifted dramatically over the previous two decades. The majority of the flood-affected lands have been converted to agriculture, with large plots dedicated to seasonal cropping. The built-up area has grown. However, it is not concentrated or clustered in one location; rather, it is dispersed in a random pattern. However, natural vegetation coverage has reduced, potentially causing soil erosion, despite the fact that precipitation patterns have been consistent over the last 30 years, with the exception of a few exceptional years, such as floods in 1991, 1993, 1996, 2000, and 2013 (Govt. of West Bengal report 2013). However, the present study can be analyzed on block level to understand the vulnerability to floods in community level so that community preparedness programs can be adopted effectively. Along with the flood susceptibility mapping, flood hazard rating may be performed to analyze the flood risk zone. Flood hazard modeling may be executed to validate the susceptibility analysis.

References

Adnan, M., Dewan, A., Zannat, K., & Abdullah, A. (2019). The use of watershed geomorphic data in flash flood susceptibility zoning: A case study of the Karnaphuli and Sangu river basins of Bangladesh. *Natural Hazards, 99*(1), 425–448. https://doi.org/10.1007/s11069-019-03749-3

Ahmad, M. (2018). Application of remote sensing and GIS for flood hazard management : A case study of Bihar (India). Contemporary. *Social Sciences, 27*(2), 69–77. https://doi.org/10.29070/27/57466

Ahmed, A., Hewa, G., & Alrajhi, A. (2021). Flood susceptibility mapping using a geomorphometric approach in South Australian basins. *Natural Hazards, 106*(1), 629–653. https://doi.org/10.1007/s11069-020-04481-z

Alam, A., Ahmed, B., & Sammonds, P. (2021). Flash flood susceptibility assessment using the parameters of drainage basin morphometry in SE Bangladesh. *Quaternary International, 575–576*, 295–307. https://doi.org/10.1016/j.quaint.2020.04.047

Arabameri, A., Rezaei, K., Cerdà, A., Conoscenti, C., & Kalantari, Z. (2019). A comparison of statistical methods and multi-criteria decision making to map flood hazard susceptibility in Northern Iran. *Science of the Total Environment, 660*, 443–458. https://doi.org/10.1016/j.scitotenv.2019.01.021

Astaras, T., Oikonomidis, D., & Mouratidis, A. (2011). *Psifiakí Chartografía kai Geografiká Systímata Pliroforión* [Digital Cartography and GIS]. Ekdóseis Dísigma [Disigma Publishing Group].

Baez-Villanueva, O., Zambrano-Bigiarini, M., Ribbe, L., Nauditt, A., Giraldo-Osorio, J., & Thinh, N. (2018). Temporal and spatial evaluation of satellite rainfall estimates over different regions in Latin-America. *Atmospheric Research, 213*, 34–50. https://doi.org/10.1016/j.atmosres.2018.05.011

Baky, M., Islam, M., & Paul, S. (2019). Flood hazard, vulnerability and risk assessment for different land use classes using a flow model. *Earth Systems and Environment, 4*(1), 225–244. https://doi.org/10.1007/s41748-019-00141-w

Bhat, M., Alam, A., Ahmad, S., Farooq, H., & Ahmad, B. (2019). Flood hazard assessment of upper Jhelum basin using morphometric parameters. *Environmental Earth Sciences, 78*(2). https://doi.org/10.1007/s12665-019-8046-1

Birkholz, S., Muro, M., Jeffrey, P., & Smith, H. (2014). Rethinking the relationship between flood risk perception and flood management. *Science of the Total Environment, 478*, 12–20. https://doi.org/10.1016/j.scitotenv.2014.01.061

Biswas, M., & Banerjee, P. (2018). Bridge construction and river channel morphology—A comprehensive study of flow behavior and sediment size alteration of the river Chel, India. *Arabian Journal of Geosciences*, 1–23. https://doi.org/10.1007/s12517-018-3789-7

Biswas, M., & Dhara, P. (2019). Evolutionary characteristics of meander cut-off—A hydromorphological study of the Jalangi River, West Bengal, India. *Arabian Journal of Geosciences, 12*, 667. https://doi.org/10.1007/s12517-019-4711-7

Bui, D. T., Ngo, P. T. T., Pham, T. D., Jaafari, A., Minh, N. Q., Hoa, P. V., & Samui, P. (2019, August). A novel hybrid approach based on a swarm intelligence optimized extreme learning machine for flash flood susceptibility mapping. *CATENA, 179*, 184–196. https://doi.org/10.1016/j.catena.2019.04.009

Chakraborty, A., & Joshi, P. (2014). Mapping disaster vulnerability in India using analytical hierarchy process. *Geomatics, Natural Hazards and Risk, 7*(1), 308–325. https://doi.org/10.1080/19475705.2014.897656

Chakraborty, S., & Mukhopadhyay, S. (2019). Assessing flood risk using analytical hierarchy process (AHP) and geographical information system (GIS): Application in Coochbehar district of West Bengal, India. *Natural Hazards, 99*(1), 247–274. https://doi.org/10.1007/s11069-019-03737-7

Chang, H., & Franczyk, J. (2008). Climate change, land-use change, and floods: Toward an integrated assessment. *Geography Compass, 2*(5), 1549–1579. https://doi.org/10.1111/j.1749-8198.2008.00136.x

Costache, R., Pham, Q., Sharifi, E., Linh, N., Abba, S., Vojtek, M., et al. (2019). Flash-flood susceptibility assessment using multi-criteria decision making and machine learning supported by remote sensing and GIS techniques. *Remote Sensing, 12*(1), 106. https://doi.org/10.3390/rs12010106

CRED, U. (2015). *The human cost of natural disasters 2015: A global perspective*. Centre for Research on Epidemiology of Disasters, Universitécatholique de . . ., 2015.

Dandapat, K., & Panda, G. (2017). Flood vulnerability analysis and risk assessment using analytical hierarchy process. *Modeling Earth Systems and Environment, 3*(4), 1627–1646. https://doi.org/10.1007/s40808-017-0388-7

Darabi, H., Choubin, B., Rahmati, O., TorabiHaghighi, A., Pradhan, B., & Kløve, B. (2019). Urban flood risk mapping using the GARP and QUEST models: A comparative study of machine learning techniques. *Journal of Hydrology, 569*, 142–154. https://doi.org/10.1016/j.jhydrol.2018.12.002

Das, S., & Sahu, A. (2017). Flood zonation mapping through RS and GIS techniques: A case study in Panskura of Purba Medinipur District, West Bengal. In S. Chatterjee (Ed.), *Indian journal of landscape systems and ecological studies* (pp. 126–135).

Das, M., Chattopadhyay, A., & Basu, R. (2017). Spatial Flood Potential Mapping (SFPM) with flood probability and exposure indicators of flood vulnerability: Case study former Jalpaiguri District, West Bengal, India. *Journal of Geography & Natural Disasters, 7*(3). https://doi.org/10.4172/2167-0587.1000210

Das, S. (2019). Geospatial mapping of flood susceptibility and hydro-geomorphic response to the floods in Ulhas basin, India. *Remote Sensing Applications: Society and Environment, 14*, 60–74. https://doi.org/10.1016/j.rsase.2019.02.006

Dawod, G., Mirza, M., & Al-Ghamdi, K. (2012). GIS-based estimation of flood hazard impacts on road network in Makkah city, Saudi Arabia. *Environmental Earth Sciences, 67*(8), 2205–2215. https://doi.org/10.1007/s12665-012-1660-9

Degiorgis, M., Gnecco, G., Gorni, S., Roth, G., Sanguineti, M., & Taramasso, A. (2012). Classifiers for the detection of flood-prone areas using remote sensed elevation data. *Journal of Hydrology, 470–471*, 302–315. https://doi.org/10.1016/j.jhydrol.2012.09.006

Dewan, A. (2013). *Floods in a megacity: Geospatial techniques in assessing hazards, risk and vulnerability*. Springer.

Dhar, O. N., & Nandargi, S. (2003). Hydrometeorological aspects of floods in India. *Natural Hazards, 28*(1), 1–33. https://doi.org/10.1023/a:1021199714487

Domakinis, C., Mouratidis, A., Voudouris, K., Astaras, T., & Karypidou, M. (2020). Flood susceptibility mapping in Erythropotamos river basin with the aid of remote sensing and GIS. *AUC Geographica, 55*(2), 149–164. https://doi.org/10.14712/23361980.2020.11

El Bastawesy, M., Attwa, M., Abdel Hafeez, T., & Gad, A. (2019). Flash floods and groundwater evaluation for the non-gauged dryland catchment using remote sensing, GIS and DC resistivity data: A case study from the Eastern Desert of Egypt. *Journal of African Earth Sciences, 152*, 245–255. https://doi.org/10.1016/j.jafrearsci.2019.02.004

Ghosh, T. (2018). Floods and people, colonial North Bengal, 1871–1922. *Studies in People's History, 5*(1), 32–47. https://doi.org/10.1177/2348448918759855

Ghosh, A., & Kar, S. (2018). Application of analytical hierarchy process (AHP) for flood risk assessment: A case study in Malda district of West Bengal, India. *Natural Hazards, 94*(1), 349–368. https://doi.org/10.1007/s11069-018-3392-y

Hu, P., Zhang, Q., Shi, P., Chen, B., & Fang, J. (2018). Flood-induced mortality across the globe: Spatiotemporal pattern and influencing factors. *Science of the Total Environment, 643*, 171–182. https://doi.org/10.1016/j.scitotenv.2018.06.197

Jarrett, R., & Tomlinson, E. (2000). Regional interdisciplinary paleoflood approach to assess extreme flood potential. *Water Resources Research, 36*(10), 2957–2984. https://doi.org/10.1029/2000wr900098

Kabenge, M., Elaru, J., Wang, H., & Li, F. (2017). Characterizing flood hazard risk in data-scarce areas, using a remote sensing and GIS-based flood hazard index. *Natural Hazards, 89*(3), 1369–1387. https://doi.org/10.1007/s11069-017-3024-y

Kale, V. S. (2004). *Floods in India: Their frequency and pattern. Coping with natural hazards: Indian context* (pp. 91–103). Orient Longman.

Kaur, H., Gupta, S., Parkash, S., Thapa, R., & Mandal, R. (2017). Geospatial modelling of flood susceptibility pattern in a subtropical area of West Bengal, India. *Environmental Earth Sciences, 76*(9). https://doi.org/10.1007/s12665-017-6667-9

Kazakis, N., Kougias, I., & Patsialis, T. (2015). Assessment of flood hazard areas at a regional scale using an index-based approach and analytical hierarchy process: Application in Rhodope–Evros region, Greece. *Science of the Total Environment, 538*, 555–563. https://doi.org/10.1016/j.scitotenv.2015.08.055

Khosravi, K., Pourghasemi, H., Chapi, K., & Bahri, M. (2016). Flash flood susceptibility analysis and its mapping using different bivariate models in Iran: A comparison between Shannon's entropy, statistical index, and weighting factor models. *Environmental Monitoring and Assessment, 188*(12). https://doi.org/10.1007/s10661-016-5665-9

Kowalzig. (2008). Climate, poverty, and justice: What the Poznań UN climate conference needs to deliver for a fair and effective global deal. *Oxfam Policy and Practice: Climate Change and Resilience*, 117–148.

Li, C., Chai, Y., Yang, L., & Li, H. (2016). Spatio-temporal distribution of flood disasters and analysis of influencing factors in Africa. *Natural Hazards, 82*(1), 721–731. https://doi.org/10.1007/s11069-016-2181-8

Mahmood, S., & Rahman, A. (2019). Flash flood susceptibility modeling using geo-morphometric and hydrological approaches in Panjkora Basin, Eastern Hindu Kush, Pakistan. *Environmental Earth Sciences, 78*(1). https://doi.org/10.1007/s12665-018-8041-y

Malik, S., Chandra Pal, S., Chowdhuri, I., Chakrabortty, R., Roy, P., & Das, B. (2020). Prediction of highly flood prone areas by GIS based heuristic and statistical model in a monsoon dominated region of Bengal Basin. *Remote Sensing Applications: Society and Environment, 19*, 100343. https://doi.org/10.1016/j.rsase.2020.100343

Mandal, S., & Sarkar, S. (2016). Overprint of neotectonism along the course of River Chel, North Bengal, India. *Journal of Palaeogeography, 5*(3), 221–240. https://doi.org/10.1016/j.jop.2016.05.004

Mojaddadi, H., Pradhan, B., Nampak, H., Ahmad, N., & Ghazali, A. H. B. (2017). Ensemble machine-learning-based geospatial approach for flood risk assessment using multi-sensor remote-sensing data and GIS. Geomatics, *Natural Hazards and Risk, 8*(2), 1080–1102. https://doi.org/10.1080/19475705.2017.1294113

Mohamed, S., & El-Raey, M. (2019). Vulnerability assessment for flash floods using GIS spatial machine-learning-based sensed data in El-Arish City, North Sinai, Egypt. *Natural Hazards, 102*(2), 707–728. https://doi.org/10.1007/s11069-019-03571-x

Mouratidis, A., & Sarti, F. (2012). Flash-flood monitoring and damage assessment with SAR data: Issues and future challenges for earth observation from space sustained by case studies from the Balkans and Eastern Europe. *Lecture Notes in Geoinformation and Cartography*, 125–136. https://doi.org/10.1007/978-3-642-32714-8_8

Mirzaei, S., Vafakhah, M., Pradhan, B., & Alavi, S. J. (2020, October 15). Flood susceptibility assessment using extreme gradient boosting (EGB), Iran. *Earth Science Informatics, 14*(1), 51–67. https://doi.org/10.1007/s12145-020-00530-0

NBFCC. (1965). *Master plan of flood control and drainage improvement 111 the catchment of river Teesta, December, 1965*. Govt. of West Bengal.

Patrikaki, O., Kazakis, N., Kougias, I., Patsialis, T., Theodossiou, N., & Voudouris, K. (2018). Assessing flood Hazard at river basin scale with an index-based approach: The case of Mouriki, Greece. *Geosciences, 8*(2), 50. https://doi.org/10.3390/geosciences8020050

Paul, A., & Biswas, M. (2019). Changes in river bed terrain and its impact on flood propagation – A case study of River Jayanti, West Bengal, India. *Geomatics, Natural Hazards and Risk*, 10(1). https://doi.org/10.1080/19475705.2019.1650124

Paul, G., Saha, S., & Hembram, T. (2019). Application of the GIS-based probabilistic models for mapping the flood susceptibility in Bansloi sub-basin of Ganga-Bhagirathi River and their comparison. *Remote Sensing in Earth Systems Sciences, 2*(2–3), 120–146. https://doi.org/10.1007/s41976-019-00018-6

Quesada Román, A. (2021). Landslides and floods zonation using geomorphological analyses in a dynamic basin of Costa Rica. *Revista Cartográfica, 102*, 125–138. https://doi.org/10.35424/rcarto.i102.901

Raha, A., & Biswas, M. (2022a). Himalayan foredeep neotectonics and deformed riverscape landforms: An integrated discussion, West Bengal, India. In H. N. Bhattacharya, S. Bhattacharya, B. C. Das, & A. Islam (Eds.), *Himalayan neotectonics and channel evolution* (Society of Earth Scientists Series). Springer. https://doi.org/10.1007/978-3-030-95435-2_11

Raha, A., & Biswas, M. (2022b). Quaternary alluvial fan dynamics of the Jaldhaka basin. *Journal of Mountain Science, 19*(8). https://doi.org/10.1007/s11629-021-7005-y

Rahman, M., Ningsheng, C., Islam, M., Dewan, A., Iqbal, J., Washakh, R., & Shufeng, T. (2019). Flood susceptibility assessment in Bangladesh using machine learning and multi-criteria decision analysis. *Earth Systems and Environment, 3*(3), 585–601. https://doi.org/10.1007/s41748-019-00123-y

Rai, P., & Mohan, K. (2014). Remote sensing data & GIS for flood risk zonation mapping in Varanasi District, India. *Forum Geografic, XIII*(1), 25–33. https://doi.org/10.5775/fg.2067-4635.2014.041.i

Rastogi, A., Thakur, P., Rao, G., Aggarwal, S., Dadhwal, V., & Chauhan, P. (2018). Integrated flood study of bagmati river basin with hydro processing, flood inundation mapping & 1-D hydrodynamic modeling using remote sensing and GIS. *ISPRS Annals of the Photogrammetry,*

Remote Sensing and Spatial Information Sciences, *IV-5*, 165–172. https://doi.org/10.5194/isprs-annals-iv-5-165-2018

Rimba, A., Setiawati, M., Sambah, A., & Miura, F. (2017). Physical flood vulnerability mapping applying geospatial techniques in Okazaki City, Aichi Prefecture, Japan. *Urban Science, 1*(1), 7. https://doi.org/10.3390/urbansci1010007

Roy, S. (2011). *Flood hazards in Jalpaiguri District and its management* (Ph.D.). University of North Bengal.

Roy, S., Bose, A., & Chowdhury, I. (2021). Flood risk assessment using geospatial data and multi-criteria decision approach: A study from historically active flood-prone region of Himalayan foothill, India. *Arabian Journal of Geosciences, 14*(11). https://doi.org/10.1007/s12517-021-07324-8

Rozalis, S., Morin, E., Yair, Y., & Price, C. (2010). Flash flood prediction using an uncalibrated hydrological model and radar rainfall data in a Mediterranean watershed under changing hydrological conditions. *Journal of Hydrology, 394*(1–2), 245–255. https://doi.org/10.1016/j.jhydrol.2010.03.021

Saaty, T. (1980). *The analytic hierarchy process: Planning, priority setting, resource allocation*. McGraw-Hill International Book Co. ISBN: 0070543712 9780070543713.

Saaty, T. (1990). How to make a decision: The analytic hierarchy process. *European Journal of Operational Research, 48*(1), 9–26. https://doi.org/10.1016/0377-2217(90)90057-I

Sahu, A. (2014). A study on Moyna basin water-logged areas (India) using remote sensing and GIS methods and their contemporary economic significance. *Geography Journal, 2014*, 1–9. https://doi.org/10.1155/2014/401324

Samanta, S., Koloa, C., Kumar Pal, D., & Palsamanta, B. (2016, August 2). Flood risk analysis in lower part of Markham river based on multi-criteria decision approach (MCDA). *Hydrology, 3*(3), 29. https://doi.org/10.3390/hydrology3030029

Sankhua, R., Sharma, N., & Garg, P. (2015). Flood management through ANN-based spatio-temporal morphological model – A potential approach for the Brahmaputra.

Sarkar, D., & Mondal, P. (2019). Flood vulnerability mapping using frequency ratio (FR) model: A case study on Kulik river basin, indo-Bangladesh Barind region. *Applied Water Science, 10*(1). https://doi.org/10.1007/s13201-019-1102-x

Şener, Ş., Sener, E., & Karagüzel, R. (2010). Solid waste disposal site selection with GIS and AHP methodology: A case study in Senirkent–Uluborlu (Isparta) Basin, Turkey. *Environmental Monitoring and Assessment, 173*(1–4), 533–554. https://doi.org/10.1007/s10661-010-1403-x

Shehata, M., & Mizunaga, H. (2018). Flash flood risk assessment for Kyushu Island. *Japan Environmental Earth Science*.

Shrestha, U., Gautam, S., & Bawa, K. (2012). Widespread climate change in the Himalayas and associated changes in local ecosystems. *PLoS One, 7*(5), e36741. https://doi.org/10.1371/journal.pone.0036741

Swain, K., Singha, C., & Nayak, L. (2020). Flood susceptibility mapping through the GIS-AHP technique using the cloud. *ISPRS International Journal of Geo-Information, 9*(12), 720. https://doi.org/10.3390/ijgi9120720

Tehrany, M., Lee, M., Pradhan, B., Jebur, M., & Lee, S. (2014). Flood susceptibility mapping using integrated bivariate and multivariate statistical models. *Environmental Earth Sciences, 72*(10), 4001–4015. https://doi.org/10.1007/s12665-014-3289-3

Tien Bui, D., Khosravi, K., Shahabi, H., Daggupati, P., Adamowski, J., Melesse, M. A., et al. (2019). Flood spatial Modeling in Northern Iran using remote sensing and GIS: A comparison between evidential belief functions and its ensemble with a multivariate logistic regression model. *Remote Sensing, 11*(13), 1589. https://doi.org/10.3390/rs11131589

Woods, R., & Sivapalan, M. (1997). A connection between topographically driven runoff generation and channel network structure. *Water Resources Research, 33*(12), 2939–2950. https://doi.org/10.1029/97wr01880

Yésou, H., Sarti, F., Tholey, N., Mouratidis, A., Clandillon, S., Huber, C., Stude R. M., & De Fraipont, P. (2013). *Addressing emergency flood mapping and monitoring of inland water*

bodies with sentinel 1–2. Expectations and perspectives. Living Planet Symposium, 9–13 September 2013, Edinburgh, UK, ESA SP-722.

Youssef, A. M., Pradhan, B., & Hassan, A. M. (2010). Flash flood risk estimation along the St. Katherine road, southern Sinai, Egypt using GIS based morphometry and satellite imagery. *Environmental Earth Sciences, 62*(3), 611–623. https://doi.org/10.1007/s12665-010-0551-1

Youssef, A., Pradhan, B., & Sefry, S. (2015). Flash flood susceptibility assessment in Jeddah city (Kingdom of Saudi Arabia) using bivariate and multivariate statistical models. *Environmental Earth Sciences, 75*(1). https://doi.org/10.1007/s12665-015-4830-8

Zhong, S., Yang, L., Toloo, S., Wang, Z., Tong, S., Sun, X., et al. (2018). The long-term physical and psychological health impacts of flooding: A systematic mapping. *Science of the Total Environment, 626*, 165–194. https://doi.org/10.1016/j.scitotenv.2018.01.041

Zhou, Z., Wang, X., Sun, R., Ao, X., Sun, X., & Song, M. (2014). Study of the comprehensive risk analysis of dam-break flooding based on the numerical simulation of flood routing. Part II: Model application and results. *Natural Hazards, 72*(2), 675–700. https://doi.org/10.1007/s11069-013-1029-8